HexaMorph: A Reconfigurable and Foldable Hexapod Robot Inspired by Origami

Wei Gao, Ke Huo, Jasjeet S. Seehra, Karthik Ramani, and Raymond J. Cipra

***Abstract*— Origami affords the creation of diverse 3D objects through explicit folding processes from 2D sheets of material. Originally as a paper craft from 17th century AD, origami designs reveal the rudimentary characteristics of sheet folding: it is lightweight, inexpensive, compact and combinatorial. In this paper, we present "HexaMorph", a novel starfish-like hexapod robot designed for modularity, foldability and reconfigurability. Our folding scheme encompasses periodic foldable tetrahedral units, called "Basic Structural Units" (BSU), for constructing a family of closed-loop spatial mechanisms and robotic forms. The proposed hexapod robot is fabricated using single sheets of cardboard. The electronic and battery components for actuation are allowed to be preassembled on the flattened crease-cut pattern and enclosed inside when the tetrahedral modules are folded. The self-deploying characteristic and the mobility of the robot are investigated, and we discuss the motion planning and control strategies for its squirming locomotion. Our design and folding paradigm provides a novel approach for building reconfigurable robots using a range of lightweight foldable sheets.**

I. INTRODUCTION

A. Origami

Origami originally was a paper-craft that affords the diversity of representative 3D objects with individual unit arrangements and explicit folding processes. In the last 40 years, different origami tessellations and structures have been described geometrically and symbolically using the underlying mathematical rules, such as flat foldability [1] and folding any polygonal shape [2]. Our study of past work in origami and folding structures shows that its applications are restricted by the following characteristics: (1) achieving a desired folding-state that renders functionality, i.e., the extended solar panel or the wrapped gift package; (2) continuous skin-based models and patterns achieved by task-oriented operations (Miura folding [3], patterns represented in airbag [4], stent [5], sandwich core structures [6] and cartons [7]); (3) recent advances in modular origami [8] use separate individual pieces of paper for each component or function. The designers still face the uncertainties of building combinatorial and kinetic structures out of single sheets of material.

B. Robotic Designs Inspired by Origami

Recent literature shows that engineers and scientists have used principles of folding for the robotic designs using programmable material [9] and displaying self-assembly capacities [10] and locomotive gaits [11]. The robot with foldable skeletons can be eased out of flat sheets of material so that it is lightweight and inexpensive, enabling batch fabrication and economies of scale. On the other hand, the advances in self-reconfigurable robots have drawn attention for assisting production manipulation [12] and planetary exploration [13]. A high degree of redundancy, modularity and complexity in functionality are encapsulated in many self-morphing robotic systems, for instance, M-TRAN [14], ATRON [15] and Miche [16].

W. Gao, K. Huo, J.S. Seehra, K. Ramani, and R.J. Cipra are with the School of Mechanical Engineering, Purdue University, West Lafayette, IN 47907, USA gao51@purdue.edu

Fig. 1. A foldable and reconfigurable starfish-like robot, "HexaMorph". (a) standing configuration. (b) "huddled" towards the center. (c) fully-deployed configuration.

In this paper, HexaMorph shown in Fig. 1, is inspired from our previous coupled folding design and fabrication theory, called Kinetogami [17]. It resembles the *Leptasterias hexactis*, known as a six-rayed starfish in the family of Asteroidea. The construct of the robot has advantages over the existing self-reconfigurable robots for the following reasons. First, in geometry, unlike most modular robotic systems with tree or open-chain architecture, there is no central body-platform in HexaMorph and each limb is interconnected within a closed-loop form. This special structure enables the robot to continuously flip inside out, exhibiting the self-deploying and space-filling characteristics. Second, the robot transforms its body among different configurations via actuating servos at different positions, rather than successively detaching and reconnecting modules from one another. And third, for manufacturability, our design methodology enables fabrication and assembly in 2D, folding and reconfiguring in 3D.

II. FOLDING SCHEME OF KINETOGAMI

Kinetogami [17] is a multi-primitive folding framework that allows folding closed-loop(s) polyhedral mechanisms (linkages) with multi-degree-of-freedom and self-deployable characteristics. The word Kinetogami is coined by the Greek root Kinetikos and the Japanese word kami, literally meaning that the polyhedral structures and mechanisms in motion are made by a single sheet of paper. Polyhedral mechanisms are the spatial mechanisms where vertices, edges and

facets of the polyhedra are embedded into kinematic linkage chains[18]. In physical kinematic linkage design, each link is modeled as a rigid body and these individual links are jointed together in closed form(s) to provide a certain determinate motion. The periodic polyhedral pairs with reflectional symmetry are called *"Basic Structural Units" (BSUs)* where adjacent hinge axes retain skew perpendicularity. The BSUs are folded in a way that each individual polyhedron is a rigid link and maintains the hinge orientations. These folded links, while structural, enclose empty volume inside. By connecting identical BSUs in serial and parallel, the resulting mechanisms can reconfigure and manifest different functions afforded by the new configuration.

In the folding scheme of Kinetogami, we model the paper creases as revolute joints (hinges), the uncreased facets as polyhedral surfaces and closed-form surfaces as kinematic linkages. Line-cuts are necessitated for silhouetting the unfolded pattern of each polyhedral linkage and the attachments are for closing and securing each physical volumetric unit as a rigid body. Our Kinetogami folding approach provides the following advantages:

1) The hinges are inherently embedded as the creases inside the 2D pattern, so that no assemblages of separate joints are needed to construct the robot.
2) The internal empty space inside BSU can be utilized for added functions, such as enclosing electronic and battery components for actuation.

A. Tetrahedral Basic Structural Units

Four triangular facets and six edges comprise a tetrahedral unit. In order to form a closed tetrahedron, each set of unfolded triangle patches needs to maintain that 1) any side length of each triangle must agree with the one to be joined from the other three triangles, and 2) the sum of angles spanned by adjacent edges emanating from the vertex must be less than 2π. If the sum is equal to 2π, a tetrahedron converts to a plane; and if greater than 2π, a tetrahedron can not be formed.

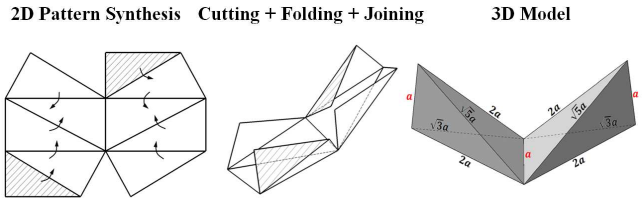

Fig. 2. Folding flattened crease-cut-attachment pattern to a single skew tetrahedral BSU.

The coupled mirror-image tetrahedra with a common hinge forms a tetrahedral BSU. When flattening each BSU, the single paper usage requires that none of any two neighboring facets overlaps upon each other. Hence, we design the hinge edges in parallel and the unfolding pattern of each current unit is in between the adjacent hinges. Fig. 2 shows the skew tetrahedral BSUs we used for this robot, where each sides' geometry are all right-angle triangles and edges are in the ratio of $1:\sqrt{3}:2:\sqrt{5}:2:1$. A closed loop of serial-connected BSUs (necessarily identical to each other) is called a *BSU ring*. More complex tetrahedral mechanisms with multiple degrees of freedom can be hierarchically achieved using serial, parallel and hybrid assemblies of BSU rings.

B. Hierarchical Construction of Tetrahedral BSUs

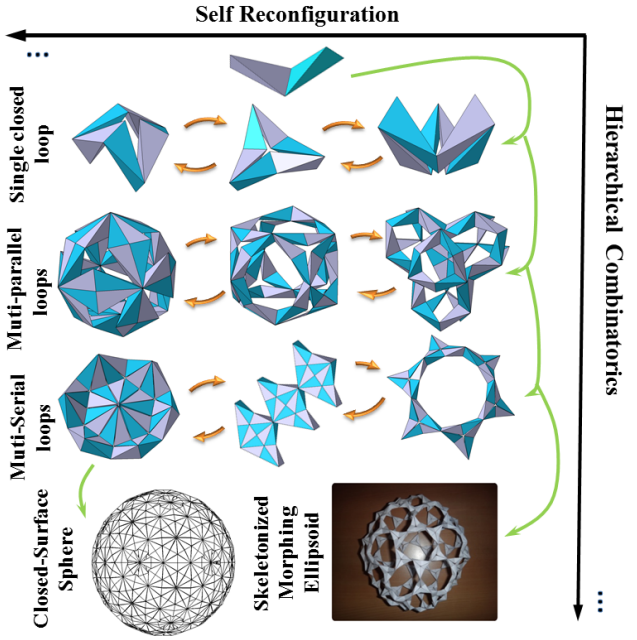

Fig. 3. A hierarchical building architecture using skew tetrahedral BSUs.

In 1929, Paul Schatz [19] first invented the single closed chain with an even number of symmetric tetrahedra. A ring hinged with 3 tetrahedral BSUs can be simplified into 6 rigid linkages, the deployable mechanism is named threefold symmetric Bricard linkage [20]. Schattschneider and Walker [21] decorated the surfaces of a single tetrahedra chain with different colors and called it Kaleidocycle. However, how to flatten and fold up the parallel mechanisms that contains multiple chains and loops, is still a challenge for engineers to synthesize and even to perceive. In our folding scheme, the skew tetrahedral BSU is geometrically selected based that the two adjacent joint axes in each unit are skew perpendicular to each other. We chain the BSUs into multiple closed loops so that each loop satisfies the plane-symmetric and trihedral linkage conditions [22]. It results in a deployable kinematic property. Fig. 3 shows that starting from a single BSU, a higher level locomotion is enabled by using serial, parallel and hybrid assemblies.

The skew tetrahedral BSU, or stBSU for short (see Fig. 3) as a basis turns out to be combinatorial in both structural and kinematic manners. The white and blue tetrahedral units reveal the reflective symmetry. Via connecting three stBSUs in a serial closed loop (3stBSU), we form a 6R Bricard linkage (see "Single closed loop" in Fig. 3). Further hinging six 3stBSUs serially yields a hexagon-like mechanism shown in "Multi-Serial-Loops" of Fig. 3. It can deploy up

to a hexagram-like mechanism with unfilled central space (see "Multi-Serial-Loops" in Fig. 3). By rearranging the mechanisms into different configurations and continuing to build identical structures cumulatively, it generates various structures and mechanisms, for example, a closed-surface sphere with overall 540 stBSUs, and a skeletonized ellipsoid with overall 216 stBSUs, shown in Fig. 3. We choose the hexagon-like mechanism shown in "Multi-Serial-Loops" of Fig. 3 as the prototype of our proposed hexapod robot.

C. Folding the Hexapod Robot using Skew Tetrahedral BSUs

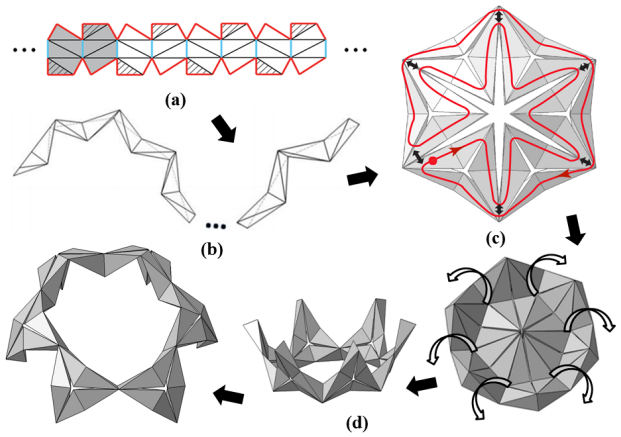

Fig. 4. (a) Linear extension of single pattern of skew tetrahedral BSU (b) skew tetrahedral BSU string (c) Eulerian cycle generation for the hexapod robot (d) deploying from hexagon-like configuration into standing stance

As discussed, we present the hexapod robot construction by stringing up 6 3stBSUs as each limb together (overall 18 skew tetrahedral BSUs) serially. By assigning the fabrication and folding principles [17] into 2D sheets of material, we first duplicate and linearly extend the single pattern of skew tetrahedral BSU (see the grey area in Fig. 4(a)) along a strip of sheet, then fold each individual pattern up in order to obtain a long BSU string shown in Fig. 4(b). The BSU string is threaded along an Eulerian cycle shown in Fig. 4(c), which starts from an arbitrary BSU and visits each of the remaining BSUs exactly once. After closing all the disconnected compound joints (illustrated as the black double arrows in Fig. 4(c)), therefore, we construct this robot shown in Fig. 4(d) with 6 limbs, each limb comprising a 3stBSU.

III. GEOMETRIC-KINEMATIC INTERPRETATION OF HEXAMORPH

In this section, the kinematics of Hexamorph is systematically parameterized along with geometric properties to interpret its continuous self-deploying motion. We further analyze the mobility of the robot to lay the groundwork for actuation and control strategy.

A. $\Phi - T$ Transformation System

Sheth and Uicker [23] presented a standard geometric terminology, called $\Phi - T$ matrices for the kinematic analysis of spatial closed-loop mechanisms. With two Cartesian coordinate frames X_{i-1}, Y_{i-1}, Z_{i-1} and U_i, V_i, W_i attaching on the n successive links, the loop closure equation with n mating joints can be written as:

$$\left[{}^{0}\Phi_1\right]\cdot\left[T_1\right]\cdots\left[{}^{n-1}\Phi_n\right]\cdot\left[T_n\right] = \sum_{i=1}^{n}\left[{}^{i-1}\Phi_i\right]\cdot\left[T_i\right] = I \quad (1)$$

where ${}^{i-1}\Phi_i$ is the joint constraint matrix and T_i is the shape matrix.

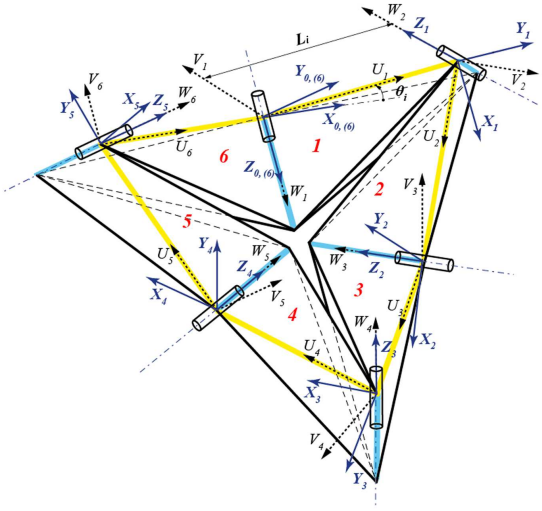

Fig. 5. $\Phi - T$ transformation matrices for individual limb.

To represent the kinematics of each single closed-loop limb using the $\Phi - T$ transformation system, we consider each skew tetrahedral unit as a rigid link (see yellow line segments in Fig. 5). Each link is skew perpendicular to its 2 adjacent hinge axes highlighted in blue in Fig. 5. Hence, the transformation matrices for each of the six joints can be written as:

$${}^{i-1}\Phi_i = \begin{bmatrix} \mathrm{C}\theta_i & -\mathrm{S}\theta_i & 0 & 0 \\ \mathrm{S}\theta_i & \mathrm{C}\theta_i & 0 & 0 \\ 0 & 0 & 1 & 0 \\ 0 & 0 & 0 & 1 \end{bmatrix}, where \quad i = 1, 2, \ldots, 6. \quad (2)$$

and the transformation matrices for each link can be written as:

$$T_{1,3,5} = \begin{bmatrix} 0 & 1 & 0 & \mathrm{L} \\ 0 & 0 & 1 & 0 \\ 1 & 0 & 0 & 0 \\ 0 & 0 & 0 & 1 \end{bmatrix}, \; T_{2,4,6} = \begin{bmatrix} 1 & 0 & 0 & \mathrm{L} \\ 0 & 0 & -1 & 0 \\ 0 & 1 & 0 & 0 \\ 0 & 0 & 0 & 1 \end{bmatrix} \quad (3)$$

The six shape parameters L are equal in length and the 6 joint variables θ_i fulfill the following conditions during the motion:

$$\theta_1 = \theta_3 = \theta_5 = A, \quad \theta_2 = \theta_4 = \theta_6 = B \quad (4)$$

By substituting the 4×4 transformation matrices into the loop closure equation (1), one can generate the geometric

relationship between the 2 joint variables A and B in each individual limb:

$$B = \sin^{-1}\left(\frac{\cos(A)}{-\cos(A)-1}\right),\ where\ -\frac{2}{3}\pi \le A \le \frac{2}{3}\pi. \quad (5)$$

B. Mobility Analysis of Individual Limb

In this section, we discuss the mobility analysis strategy of the robot using the system coefficient matrix [23]. Earlier efforts on the mobility determination of rigid-body mechanisms goes back to Chebyshev [24], Grübler [25], and Hunt[26], etc. These fundamental approaches are based on subtracting the overall constraints from the degree of freedoms of all links, but neglecting certain special geometric conditions such as perpendicularity and parallelism which the mechanical system possesses. In every $\Phi - T$ transformation system, the number of independent inputs q is equal to the degree of freedom, m. By using the chain rule, the time derivative of ith joint's variable θ_i can be derived as:

$$\dot{\theta}_i = \sum_{j=1}^{m} \frac{\partial \theta_i}{\partial q_j}\,\dot{q}_j = \sum_{j=1}^{m} \theta'_{ij}\,\dot{q}_j \quad (6)$$

where θ'_{ij} denotes $\frac{\partial \theta_i}{\partial q_j}$ and $\dot{q}_j$ is the time derivative of jth independent input. By differentiating the loop closure equation with respect to q_j, i.e., with respect to any of potential inputs, and substituting the following equation (Q_i is the derivative operation matrix):

$$\frac{\partial \Phi_i}{\partial q_j} = Q_i\,\Phi_i\,\theta'_{ij} \quad (7)$$

the derivative of loop closure equation is derived as follows:

$$\begin{aligned}
&[{}^0A_1\,Q_1\,{}^1A_2 \cdots {}^nA_1\,{}^1A_0]\theta'_{1j}\,\dot{q}_j + \\
&[{}^0A_1\,{}^1A_2\,Q_2\,{}^2A_3 \cdots {}^nA_1\,{}^1A_0]\theta'_{2j}\,\dot{q}_j + \cdots + \\
&[{}^0A_1\,{}^1A_2 \cdots Q_n\,{}^nA_1\,{}^1A_0]\theta'_{nj}\,\dot{q}_j = 0
\end{aligned} \quad (8)$$

We define that $D_i = {}^0A_i\,Q_i\,{}^0A_i^{-1} = {}^0A_i\,Q_i\,{}^iA_0$, so that equation (8) can be rearranged as:

$$D_1\theta'_{1j}\,\dot{q}_j + D_2\theta'_{2j}\,\dot{q}_j + \cdots + D_n\theta'_{nj}\,\dot{q}_j = 0 \quad (9)$$

Since the joint constraint matrix is orthogonal and Q is anti-symmetric, the D matrix has only 6 independent elements. The compact form of equation (8) can be derived out as:

$$\begin{bmatrix} D_1(2,1) & \cdots & D_n(2,1) \\ D_1(3,1) & \cdots & D_n(3,1) \\ D_1(4,1) & \cdots & D_n(4,1) \\ D_1(2,3) & \cdots & D_n(2,3) \\ D_1(2,4) & \cdots & D_n(2,4) \\ D_1(3,4) & \cdots & D_n(3,4) \end{bmatrix} \begin{Bmatrix} \theta'_{1j} \\ \theta'_{2j} \\ \cdot \\ \cdot \\ \cdot \\ \theta'_{nj} \end{Bmatrix} = N \begin{Bmatrix} \theta'_{1j} \\ \theta'_{2j} \\ \cdot \\ \cdot \\ \cdot \\ \theta'_{nj} \end{Bmatrix} = \mathbf{0} \quad (10)$$

in which N is called the system coefficient matrix of a mechanical system and the degree-of-freedom of the system can be obtained as:

$$m = n - rank(N) \quad (11)$$

By implementing the system coefficient matrix for an individual limb, we attain its representation in a reduced row echelon form shown as below:

$$N = \begin{bmatrix} 1 & 0 & 0 & 0 & 0 & \frac{\sin B(\cos A+1)}{\sin A(\cos B+1)} \\ 0 & 1 & 0 & 0 & 0 & -1 \\ 0 & 0 & 1 & 0 & 0 & \frac{-\sin B(\cos A+1)(\cos A+\cos B+\cos A\,\cos B-1)}{\sin A(\cos B+1)} \\ 0 & 0 & 0 & 1 & 0 & \cos A+\cos B+\cos A\,\cos B-1 \\ 0 & 0 & 0 & 0 & 1 & \frac{\sin B(\cos A+1)}{\sin A(\cos B+1)} \\ 0 & 0 & 0 & 0 & 0 & 0 \end{bmatrix} \quad (12)$$

The mobility of each individual limb accordingly is $m = 6 - 5 = 1$.

C. Topology Graph and Mobility of HexaMorph

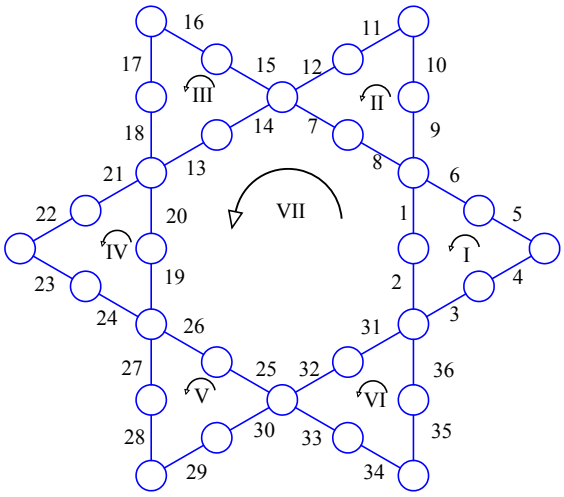

Fig. 6. Topology graph of the starfish-like hexapod Robot.

As for the system coefficient matrix N of a multi-closed-loop mechanical system, each column corresponds to an individual joint variable and each 6 rows represent an independent loop. The number of independent loops λ in a mechanism is determined using the Euler formula:

$$\lambda = n - l + 1 \quad (13)$$

where n is the number of joints and l is the number of the links. For the proposed robot in this paper, λ is 7 given that $n = 42, l = 36$. We further assemble 7 independent loops into an overall 42 by 42 system coefficient matrix. 7 independent loops are listed as below and illustrated in a topology graph shown in Fig. 6, where tetrahedral links are denoted by edges ($-$) and hinge joints are denoted by circles ($\circ$).

- Loop I: links $1-2-3-4-5-6$
- Loop II: links $7-8-9-10-11-12$
- Loop III: links $13-14-15-16-17-18$
- Loop IV: links $19-20-21-22-23-24$
- Loop V: links $25-26-27-28-29-30$
- Loop VI: links $31-32-33-34-35-36$
- Loop VII: links $2-1-8-7-14-13-20-19-26-25-32-31$

The numerical results of the rank analysis indicates that the mobility of the robot $m = 42 - 35 = 7$ for any general configuration, while the instantaneous mobility could vary in special geometric conditions and different singular configurations.

IV. DESIGN, FABRICATION AND MOTION PLANNING

A. Substrate and Electronics Design

3mm-thick corrugated cardboards are used as the substrate surfaces for the robot. Each limb in its compact volume is $0.33m \times 0.35m \times 0.38m$. The robot's net weigh is 0.765 kg with only the cardboard tetrahedral modules, and overall 2.72 kg including all the functional components. After creating the folds, cuts and snap-fits on 2D aforementioned stBSU pattern, we lay down and preassemble the electronic components on the flat.

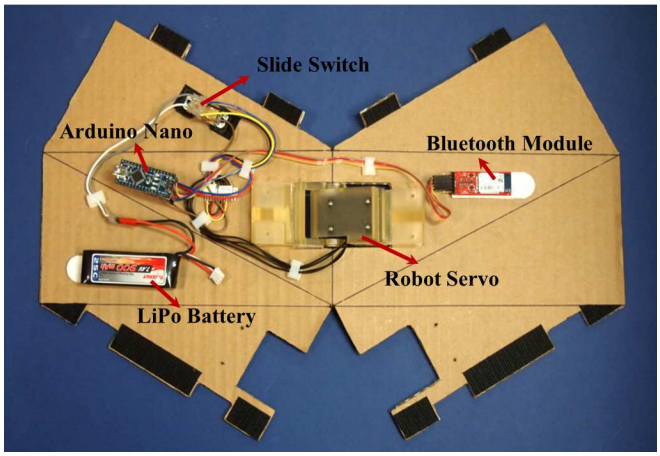

Fig. 7. Electronics layout on a single skew tetrahedral BSU pattern.

Fig. 7 shows the electronics layout on a single skew tetrahedral BSU pattern. Our electronics design for HexaMorph comprises four major components: the PC for motion planning and running GUI, 1 Arduino Nano for motion control, 1 Bluetooth module for wireless communication between PC and Arduino, and 12 robot servos for actuation and position sensing.

Fig. 8(a) further shows an overall flattened strip containing 18 periodic stBSU patterns and electronic components on the pattern. The first row shown in Fig. 8(a) indicates the 2D pattern of the stBSU string that travels the inner loop VII shown in Fig. 6. Folding the patterns in the second and third rows together constructs the rest of stBSU string in the Eulerian cycle.

We place 12 HerkuleX DRS-0101 robot servos at each hinge joint inside the inner loop, shown in Fig. 8(b). Six servos labeled "A" are inside each limb and the remaining six labeled "B" sit between 2 adjacent limbs. The resulting redundant actuation is needed to assist the robot passing through the singular configurations and balancing the torque due to the symmetry in structure. To assist in planning the associated complex joint motions, CATIA simulation is used

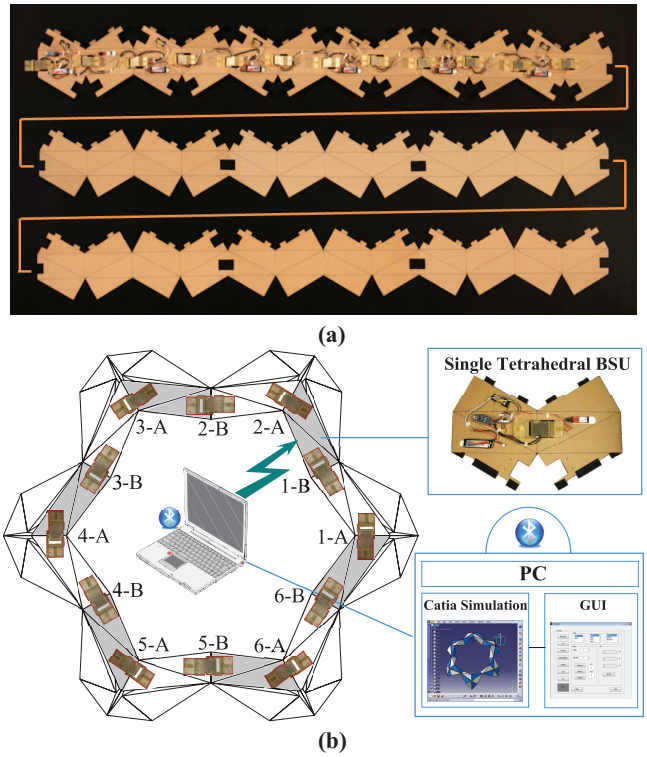

Fig. 8. (a) Overall 2D pattern with electronic components. (b) system pipeline and control strategy.

to design the reconfiguration and generate joint angles. The Arduino Nano processes all the motion sequences sent from the PC and distributes into 12 servos. When considering the modularity of each single loop, 2 adjacent servos coupled inside each tetrahedral BSU are powered with 1 Tenergy Li-Po battery (7.4v, 900mAh). Twelve daisy-chained robot servos together process different motion planning synchronously. Therefore, by closing each BSU and each individual loop up, we complete the fabrication and assembly for the hexapod robot.

B. Reconfiguration Design and Motion Control

Biologically-inspired robotics [27] and biorobotics design [28] involve endeavors of adopting the understanding of animal behaviors and embedding resemblant flexibility in robots. In this section, we propose 2 reconfiguration patterns for the hexapod tetrahedral robot: self-deploying and locomotive squirming.

Self-deploying: Nature employs efficient, elegant patterns and strategies of deploying, for instance, the petals of morning glory flower unfold from the bud and curl up back. As discussed in Section 2, both the individual single-closed-loop limbs and the multi-closed-loop robot are capable of self-deploying continuously from inside out since the mechanisms satisfy plane symmetric and trihedral linkage conditions. Twelve servos are synchronously operated to employ this motion. Starting from a standing posture shown in Fig. 9(a), the hexapod robot deploys its initial configuration internally through the fully-deployed

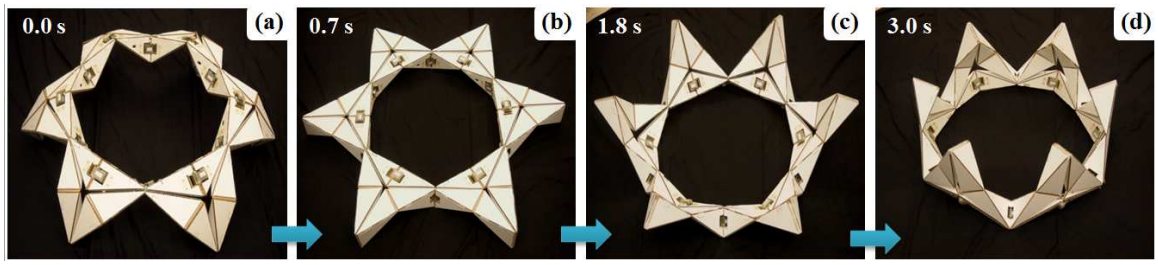

Fig. 9. Sequences of self-deploying motion. (a-b) moves from initial standing configuration to the fully-deployed configuration. (c-d) closes up to a smaller envelope volume.

configuration on the ground (see Fig. 9(b)), then towards the final "bristled" configuration (see Fig. 9(d)). This particular type of reconfiguration allows the robot to transform from a functioning stance containing stretched limbs to a storage or packaging stance with compact envelope volume. The deploying motion takes 3 seconds and can be operated on the flooring of multiple materials such as tile, wood, bamboo and plastic.

Squirming: The second reconfiguration designed for the robot is locomotive. We decompose the hexapods into one forelimb, four middle limbs and one hindlimb towards any orientation around the body. A squirming sequence comprised of 2 steps is shown in Fig. 10. After fully deploying its "huddled" body on the ground (see Fig. 11(a-c)), the special geometry reduces its mobility to 3 and six servos between 2 adjacent limbs start driving the robot to squirm forward and

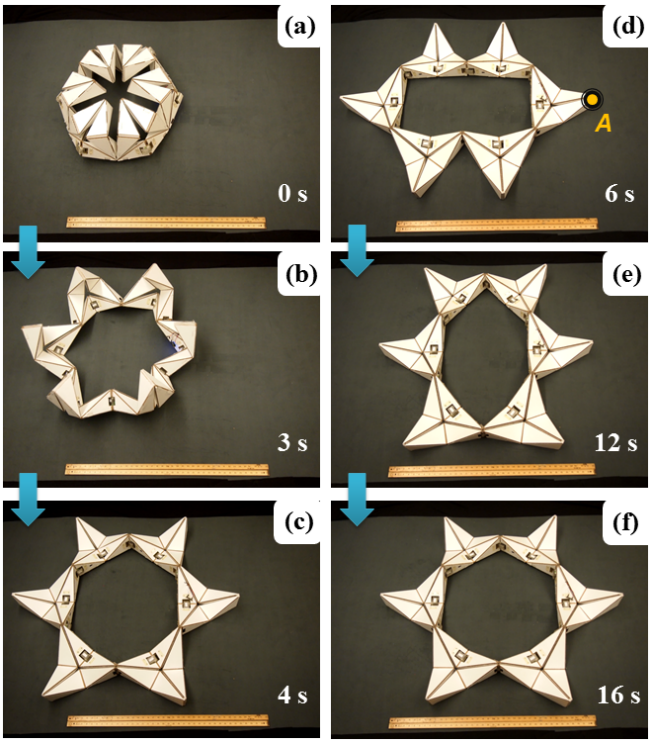

Fig. 10. Sequences of locomotive squirming motion. (a-c) opens its body till all limbs are stretched. (c-d) drives one limb while anchoring another one in order to squirm.

balance the toque. The robot first moves the forelimb forward while anchoring the hindlimb, shown in Fig. 10(d). The whole skeleton is stretched along the squirming direction. The robot then pulls the hindlimb to slide forward while anchoring the forelimb (see Fig. 10(e)), so that the skeleton contracts back to the original configuration. The overall motion proceeds like a squirming inchworm.

A one-way friction solution was applied to ensure that the moving and anchoring can happen simultaneously along the same direction. We use One-way Glide^{TM}where the tilted inner fibers allows the surface to slide in one direction only and resist sliding back. Fig. 11(a,b) shows the displacement and velocity of the front tip of the robot (illustrated as point "A" in Fig. 10(d)) over time. The displacement during each advance stroke is measured to be 200mm followed by 40 % backward-slip motion due to the friction. The maximum velocity of the robot is 240mm/s. Whenever the robot reaches the initial regular hexagram-like configuration, it is capable of converting the squirming direction by rearranging the functions of each limb. A video of more details of the robot can be accessed at: `https://engineering.purdue.edu/cdesign/wp/?p=2215`.

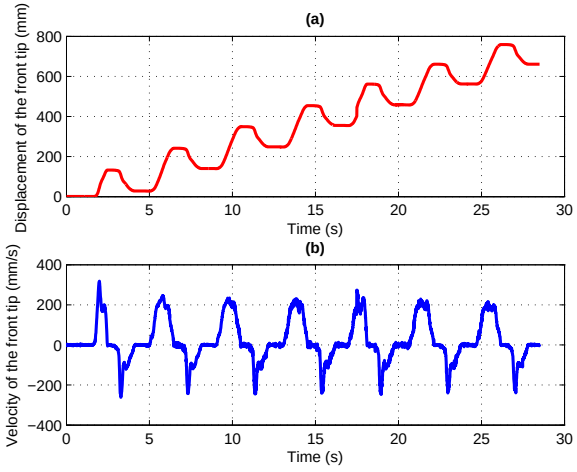

Fig. 11. (a) The displacement of the robot front tip "A". (b) the velocity of the robot front tip "A".

V. CONCLUSIONS AND FUTURE WORK

In this paper, we present HexaMorph, a novel hexapod robot design inspired by Origami. The capability of our

folding scheme enables a variety of mechanical and robotic designs by simply assembling substrate pattern and functional components on 2D, and folding and reconfiguration in 3D. The explicit 2D fabrication layout and construction rules are parameterized to ensure a continuous folding for our proposed robot. We also analyze the kinematic properties for both single- and multi-closed-loop tetrahedral mechanisms and propose two unique reconfiguration motions for HexaMorph: self-deploying and locomotive squirming.

Our future work will further explore lightweight materials with improved mechanical properties at substrates and hinges, and improve the one-friction strategy to provide stronger resisting force and avoid backward slippage. In addition, a thorough understanding of singularity of the robot is needed for an optimal selection of the number of inputs. Due to HexaMorph's capability of performing reconfiguration, we envision that the robot is capable of adjusting its body frequently in an adaptive manner to provide a wide range of movements. We will implement more body-lifting and locomotion gaits for use in the potential applications of deployment, search, and reconnaissance.

ACKNOWLEDGMENT

The authors of this paper would like to acknowledge the support by Donald W. Feddersen Chair professorship for funding this research.

REFERENCES

[1] E. M. Arkin, M. A. Bender, E. D. Demaine, M. L. Demaine, J. S. Mitchell, S. Sethia, and S. S. Skiena, "When can you fold a map?" *Computational Geometry*, vol. 29, no. 1, pp. 23–46, 2004.

[2] E. D. Demaine, M. L. Demaine, and J. S. Mitchell, "Folding flat silhouettes and wrapping polyhedral packages: New results in computational origami," *Computational Geometry*, vol. 16, pp. 105–114, 1999.

[3] K. Miura, "The science of miura-ori: A review," in *4th International Meeting of Origami Science, Mathematics and Education*, R. J. Lang, Ed. A K Peters, 2009, pp. 87–100.

[4] R. Hoffman, "Airbag folding: Origami design application to an engineering problem," in *3rd International Meeting of Origami Science, Mathematics, and Education*, Asilomar, CA.

[5] Z. You and K. Kuribayashi, "A novel origami stent," in *Proceedings of Summer Bioengineering Conference*, Key Biscayne, FL, 2003.

[6] S. Fischer, K. Drechsler, S. Kilchert, and A. Johnson, "Mechanical tests for foldcore base material properties," *Composites: PartA*, 2009.

[7] G. Mullineux, J. Feldman, and J. Matthews, "Using constraints at the conceptual stage of the design of carton erection," *Mechanism and Machine Theory*, vol. 45, no. 12, pp. 1897–1908, 2010.

[8] R. Gurkewitz and B. Arnstein, *Multimodular origami polyhedra: archimedeans, buckyballs, and duality*. Dover, New York, 2003.

[9] E. Hawkes, B. An, N. Benbernou, H. Tanaka, S. Kim, E. D. Demaine, D. Rus, and R. J. Wood, "Programmable matter by folding," *Proceedings of the National Academy of Sciences of the USA*, vol. 107, pp. 12 441–12 445, 2010.

[10] S. M. Felton, M. T. Tolley, C. D. Onal, D. Rus, and R. J. Wood, "Robot self-assembly by folding: A printed inchworm robot," in *Proc. IEEE International Conference on Robotics and Automation (ICRA'13)*, Karlsruhe, Germany, May 2013, pp. 277–282.

[11] J. Koh and K. Cho, "Omegabot: Crawling robot inspired by ascotis selenaria," in *Proc. IEEE International Conference on Robotics and Automation (ICRA'10)*, Alaska, USA, May 2010, pp. 109–114.

[12] T. Fukuda and S. Nakagawa, "Approach to the dynamically reconfigurable robotic system," in *Proceedings of IEEE International Conference on Robotics and Automation*, vol. 3, 1988, pp. 1581–1586.

[13] S. Curtis, M. Brandt, G. Bowers, G. Brown, C. Cheung, C. Cooperider, M. Desch, N. Desch, J. Dorband, K. Gregory, K. Lee, A. Lunsford, F. Minetto, W. Truszkowski, R. Wesenberg, J. Vranish, M. Abrahantes, P. Clark, T. Capon, M. Weaker, R. Watson, P. Olivier, M. L. Rilee, and G. NASA Goddard Space Flight Center, "Tetrahedral robotics for space exploration," *Aerospace and Electronic Systems Magazine, IEEE*, vol. 22, pp. 22–30, 2007.

[14] S. Murata, E. Yoshida, A. Kamimura, H. Kurokawa, K. Tomita, and S. Kokaji, "M-tran: Self-reconfigurable modular robotic system," *IEEE/ASME Transactions on Mechatronics*, vol. 7, no. 4, pp. 431–441, 2002.

[15] M. W. Jorgensen, E. H. Ostergaard, and H. H. Lund, "Modular atron: modules for a self-reconfigurable robot," *Intelligent Robots and Systems*, vol. 2, pp. 2068–2073, 2004.

[16] K. Gilpin, K. Kotay, D. Rus, and I. Vasilescu, "Miche: modular shape formation by self-disassembly," *International Journal of Robotics Research*, vol. 27, pp. 345–372, 2008.

[17] W. Gao, K. Ramani, R. Cipra, and T. Siegmund, "Kinetogami: a reconfigurable, combinatorial, and printable sheet folding," *Journal of Mechanical Design*, vol. 135, no. 11, 2013.

[18] M. Goldberg, "Polyhedral linkages," *National Mathematics Magazine*, vol. 16, no. 7, pp. 323–332, 1942.

[19] P. Schatz, "Rhythmusforschung und technik," *Stuttgart:Verlag Freies Geistesleben*, 1998.

[20] Y. Chen, Z. You, and T. Tarnai, "Threefold-symmetric bricard linkages for deployable structures," *International Journal of Solids and Structures*, vol. 42, no. 8, pp. 2287–2301, 2005.

[21] D. Sehattsehneide and W. Walker, *M.C.Eseher Kalerdoeycels*. BallantineBooks, NewYork, 1977.

[22] Y. Chen and Z. You, "Spatial overconstrained linkages - the lost jade," *History of Mechanism and Machine Science*, vol. 15, pp. 535–550, 2012.

[23] P. N. Sheth and J. J. Uicker, "A generalized symbolic notation for mechanisms," *Journal of Engineering for Industry*, vol. 93, pp. 102–112, 1971.

[24] P. Chebychev, "Théorie des mécanismes connus sous le nom de parallélogrammes, 2éme partie," in *Mémoires présentés à l'Académie imperiale des sciences de Saint-Pétersbourg par divers savants*, 1869.

[25] M. Grübler, *Getriebelehre: Eine Theorie Des Zwanglaufes Und Der Ebenen Mechanismen*. Springer, Berlin, 1917.

[26] K. Hunt, *Kinematic Geometry of Mechanisms*. Oxford University Press, Oxford, 1978.

[27] R. Pfeifer, M. Lungarella, and F. Lida, "Self-organization, embodiment, and biologically inspired robotics," *Science*, vol. 318, pp. 1088–1093, 2007.

[28] R. E. Ritzmann, R. D. Quinn, J. T. Watson, and S. N. Zill, "Insect walking and biorobotics: A relationship with mutual benefits," *BioScience*, vol. 50, no. 1, pp. 23–33, 2000.